Friction **11**(3): 425–440 (2023)
https://doi.org/10.1007/s40544-022-0614-9
ISSN 2223-7690
CN 10-1237/TH

RESEARCH ARTICLE

Lubrication mechanism of a strong tribofilm by imidazolium ionic liquid

Wei SONG[1,2], Jie ZHANG[1], Sophie CAMPEN[1], Jincan YAN[2,3], Hongbing JI[2,4], Janet S. S. WONG[1,*]

[1] *Department of Mechanical Engineering, Imperial College London, London SW7 2AZ, UK*

[2] *Fine Chemical Industry Research Institute, School of Chemistry, Sun Yat-sen University, Guangzhou 510275, China*

[3] *School of Chemical and Environmental Engineering, Shanghai Institute of Technology, Fengxian, Shanghai 201418, China*

[4] *School of Chemical Engineering, Guangdong University of Petrochemical Technology, Maoming 525000, China*

Received: 05 July 2021/ Revised: 01 October 2021 / Accepted: 03 March 2022

Abstract: Friction modifiers (FMs) are surface-active additives added to base fluids to reduce friction between rubbing surfaces. Their effectiveness depends on their interactions with rubbing surfaces and may be mitigated by the choice of the base fluid. In this work, the performance of an imidazolium ionic liquid (ImIL) additive in polyethylene-glycol (PEG) and 1,4-butanediol for lubricating steel/steel and diamond-like-carbon/diamond-like carbon (DLC–DLC) contacts were investigated. ImIL-containing PEG reduces friction more effectively in steel–steel than DLC–DLC contacts. In contrast, adding ImIL in 1,4-butanediol results in an increase in friction in steel–steel contacts. Results from the Raman spectroscopy, X-ray photoelectron spectroscopy (XPS), and focused ion beam-transmission electron microscopy (FIB-TEM) reveal that a surface film is formed on steel during rubbing in ImIL-containing PEG. This film consists of two layers. The top layer is composed of amorphous carbon and are easily removed during rubbing. The bottom layer, which contains iron oxide and nitride compound, adheres strongly on the steel surface. This film maintains its effectiveness in a steel–steel contact even after ImIL additives are depleted. Such film is not observed in 1,4-butanediol where the adsorption of ImIL is hindered, as suggested by the quartz crystal microbalance (QCM) measurements. No benefit is observed when the base fluid on its own is sufficiently lubricious, as in the case of DLC surfaces.

This work provides fundamental insights on how compatibilities among base fluid, FM, and rubbing surface affect the performance of IL as surface active additives. It reveals the structure of an ionic liquid (IL) surface film, which is effective and durable. The knowledge is useful for guiding future IL additive development.

Keywords: ionic liquid (IL); polyethylene-glycol (PEG); friction modifiers (FMs); tribofilm

1 Introduction

Friction and wear are crucial for energy efficiency and durability of engineering components. They can be managed by using high-performance lubricants [1–3]. Friction modifiers (FMs) are additives commonly used in lubricants to reduce friction, especially when contact between rubbing surfaces is expected [4, 5]. In general, the effectiveness of an FM is partly influenced by its interaction with rubbing surfaces and the nature of its tribofilm [5]. FMs have been shown to adsorb on surfaces in many ways including electrostatic interaction, hydrogen bonding interaction, and coordination interaction. A tribofilm is formed subsequently during rubbing to effectively reduce friction [6–9].

Ionic liquids (ILs) are molten salts at room temperature. Some of their physiochemical properties, like low melting point, low volatility, and non-flammability [10, 11], are desirable for lubrication. As

* Corresponding author: Janet S. S. WONG, j.wong@imperial.ac.uk

they are charged in a solvent and often have favourable interactions with metal surfaces, they have been employed as novel FMs in many applications [12–15]. Among the reported ILs, imidazolium-based ILs have attracted the most research interest because of its flexibility in molecular design and ease of synthesis [11, 16]. Note that imidazolium-based ILs contain nitrogen, an active element that is widely believed to promote tribofilm formation [11].

The effectiveness of ILs might be reduced due to antagonistic effects between ILs and other additives in lubricants [17–19]. For example, the addition of polyisobutylene succinimide (PIBSI) in IL-containing lubricants can result in competitive adsorption on surfaces [20]. Considering potential interactions between IL FMs and base fluids, their compatibility should be examined. Also note that the interactions between FMs and rubbing surfaces govern the properties of tribofilms [21]. Therefore, it is important to investigate the compatibility between FMs and the tribo-pair surface.

In this work, we seek to shed light on the following:

1) Would a base fluid compete against an IL on surface adsorption? How does the interaction between an IL and a base oil affect the IL performance?

2) Is the effectiveness of an IL additive surface-specific?

The adsorption behavior of an IL was examined using the quartz crystal microbalance with dissipation monitoring (QCM-D). Rubbing tests were conducted using a sphere-on-flat reciprocating tribometer. The formation of tribofilms during rubbing was monitored by electrical contact resistance (ECR). Surface analysis was employed to investigate the chemical nature and morphology of the tribofilm.

2 Materials

The effectiveness of an imidazolium ionic liquid (ImIL) FMs was evaluated in two base fluids, polyethylene-glycol (PEG) and 1,4-butanediol, and two rubbing surfaces (steel and diamond-like-carbon (DLC)). PEG and 1,4-butanediol, with dielectric constants of 12.4 and 30.9 F/m, respectively [22], may interact differently with FMs and rubbing surface [23]. Steel and DLC have different chemical reactivity [24], thus resulting in different IL tribofilms. Chemical structures of ImIL, PEG, and 1,4-butanediol are shown in Fig. 1.

1-methylimidazole (99%), (3-chloropropyl) trimethoxysilane (≥ 97%), anhydrous N,N-dimethylformamide (DMF, 99.8%), anhydrous diethyl ether (99.7%), PEG (number average molecular weight M_n = 400 g/mol, Fig. 1(b)), 1,4-butanediol (98%, Fig. 1(c)), and 1,3-proponediol (98%, Fig. 1(d)) were purchased from Sigma-Aldrich, and used as received. The ImIL, as shown in Fig. 1(a), was synthesized according to Ref. [25], with details described in S1 in the Electronic Supplementary Material (ESM) (note that figures, tables, and sections with a prefix "S" are in the ESM). ^{1}H nuclear magnetic resonance (NMR) spectrum of the synthesized ImIL was obtained from a spectrometer (Jeol 400 MHz) using deuterated dimethyl sulfoxide (DMSO-d6) as the solvent and tetramethylsilane as the internal standard. High-resolution mass spectrum (MS) was acquired by the electrospray–time of flight (ES–TOF) mass spectrometer (LCT Premier, Waters Corporation) with positive mode. Both ^{1}H NMR (Fig. S1-1 in the ESM) and MS (Fig. S1-2 in the ESM) spectra are in good agreement and confirm the molecular structure of ImIL.

Test lubricants containing 5 wt% of ImIL were prepared. Their viscosities, as determined by a rheometer with a coaxial cone-plate geometry (DHR-1, TA instrument), remain relatively constant in the range of shear rates from 10 to 10,000 s^{-1}. The viscosities of the base fluids with and without ImIL were similar (Fig. 2).

Balls and disks for friction tests were made of AISI 52100 steel and DLC-coated steel. They were provided by PCS instruments. Note that the thickness of DLC on steel was around 2 μm. Hence steel and DLC-coated steel are assumed to have the same mechanical properties, listed in Table 1. The diameter of balls

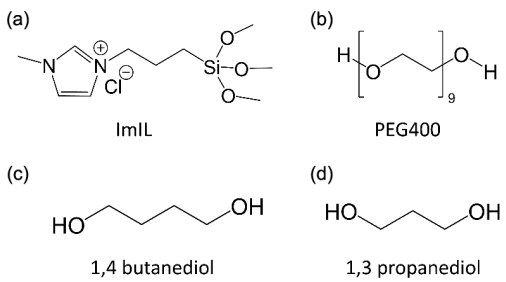

Fig. 1 Chemical structures of (a) ImIL, (b) PEG400, (c) 1,4-butanediol, and (d) 1,3-propanediol.

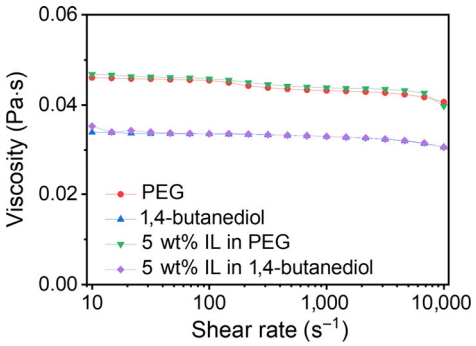

Fig. 2 Viscosities of PEG and 1,4-butanediol with and without ImIL at different shear rates.

Table 1 Mechanical properties of the test specimens.

	Steel	DLC-coated steel
Elastic modulus (GPa)	207	207
Poisson's ratio	0.3	0.3
Vickers Hardness (HV)	800	800
RMS surface roughness, *Rq* (nm)	16.8	23.2

was 6 mm. The diameter and the thickness of disks were 10 and 3 mm, respectively. The samples were rinsed in toluene and ultra-sonicated for 30 min. They were then rinsed with isopropanol (IPA), followed by drying with compressed air before friction tests.

3 Methods

3.1 Tribological test

Friction tests were conducted using a high-frequency reciprocating rig (HFRR; PCS Instruments), a ball-on-disk tribometer where a ball in reciprocating motion is pressed against a stationary disc. ECR, which measures the electrical resistance between the two rubbing surfaces and is an effective way to monitor tribofilm formation during friction [26], was recorded together with friction coefficients. All tests were conducted at 40 °C. The test conditions of different liquids were determined based on their viscosities, as shown in Table 2. Using Dowson and Hamrock's equations [27], properties of steel (Table 1), and viscosities of test fluids (Fig. 2 and Table 2), the estimated average central film thicknesses of all tested fluids in conditions listed in Table 2 are around 30 nm. Hence, the ratios of lubricant film thickness h to surface roughness were about 1.2 for steel–steel and 0.9 for DLC–DLC contacts, suggesting that tests were performed in a mixed to boundary lubrication regime [27], i.e., some asperity–asperity contacts are expected during rubbing.

All tests were repeated 3 times. Results were reproducible. All samples were rinsed with IPA after tests for further examinations.

3.2 Adsorption measurements

Interactions between constituents of test lubricants and rubbing surfaces were investigated using the QCM-D (QSense Explorer, Biolin Scientific). Fe_2O_3-coated and amorphous carbon-coated quartz sensors, with a resonance frequency f of 5 MHz, were used to represent steel and DLC-coated steel surfaces.

Tests were conducted in a flow cell where test solutions were allowed into the cell at a flow rate of 0.48 mL/s at 40 °C. Before a QCM-D adsorption test, both the flow cell and the sensor were rinsed in IPA and ultra-sonicated for 30 min, and then dried using compressed air. In each test, the frequency shift Δf_1 of the oscillating quartz sensor at its fundamental frequency and its odd overtone Δf_n of n = 3 (15 MHz), 5 (25 MHz), 7 (35 MHz), 9 (45 MHz), 11 (55 MHz), and 13 (65 MHz), were recorded. Note that a change in resonance frequency Δf can be attributed to the

Table 2 Viscosities and friction test conditions of different base fluids.

Base fluid	Density (g/cm^3)	Viscosity (mPa·s)	Frequency (Hz)	Stroke length (mm)	Load (N)
PEG	1.108	43.403	100	1	7.92
5 wt% ImIL-containing PEG	1.115	45.106	100	1	7.92
1,4-butanediol	1.003	33.398	100	1	7.92
5 wt% ImIL-containing 1,4-butanediol	1.013	33.429	100	1	7.92
1,3-propanediol	1.040	22.045	120	1	7.92
IL	—	2,490	10	0.25	7.92

surface adsorption $\Delta f_{\text{adsorption}}$, liquid loading $\Delta f_{\text{liquid loading}}$, and liquid trapping Δf_{liquid} [28, 29]. The liquid loading effect on Δf can be calculated and removed according to the reported method [28, 29]. Since the surfaces of QCM sensors are quite smooth (Ra = 0.70 nm), the effect of liquid trapping is assumed to be eligible. Note that the high viscosity of the base fluids can dampen the amplitudes of sensor oscillation, causing the sensor response to be noisy. For this reason, while results from all overtones were recorded, the discussion here will focus on Δf_n of $n = 3$, i.e., Δf_3. Same conclusion is reached for all Δf_n. Tests under each test condition were repeated at least twice, and the results were reproducible.

To investigate the interaction between the base fluids and the sensor surfaces, aqueous solutions of base fluids were prepared. A baseline was firstly obtained by flowing de-ionised water into the flow cell. Once a stable baseline was achieved, aqueous solutions of base fluids with progressively higher concentrations were allowed into the flow cell. The flow cell was rinsed with water in between solutions of different concentrations. Δf during rinsing indicates that the amount of base fluid molecules remained on the sensor surface due to the flow of the precedent solution.

For the adsorption tests of IL-containing fluids, a baseline was firstly obtained with IPA. A neat base fluid was then pumped into the flow cell, followed by IL-containing base fluid. The cell was then rinsed with the neat base fluid.

3.3 Surface characterizations

The topography of worn surface was examined by a white light interferometer (Bruker, ContourGT-X 3d Optical Profiler). The height and lateral force images of wear tracks were obtained with an atomic force microscope (AFM; Bruker Multimode AFM with Nanoscope V controller) in contact mode. A triangular cantilever composed of non-conductive silicon nitride with a free resonant frequency of 23 kHz and a spring constant of 0.12 N/m was employed during the AFM test.

Worn surfaces were examined by a Raman spectroscope with a 532 nm laser (WITec alpha300 RA) and X-ray photoelectron spectroscopy (XPS; Thermo Fisher, K-Alpha spectrophotometer). A cross-section of the worn surface was obtained by the focused ion beam (FIB), and then observed with the transmission electron microscopy (TEM; Tecnai F20). A protective Pt layer was deposited on the wear track before the FIB process.

4 Results and discussion

4.1 Tribological performance of IL

The friction coefficients of PEG with and without ImIL and their corresponding ECR in steel–steel contacts during friction tests are presented in Figs. 3(a) and 3(b), respectively. Results from an average of 3 tests are in Fig. S2 in the ESM.

PEG gives a maximum friction coefficient $\mu_{\max} \approx 0.12$ at time $t \approx 7$ min. Its friction coefficient then decreases before reaching a stable value of $\mu_{ss} \approx 0.11$ at $t \approx 28$ min. The introduction of 1 wt% ImIL FM reduces $\mu_{\max}$ and μ_{ss} by 17.6% ($\mu_{\max} \approx 0.1$) and 14.4% ($\mu_{ss} \approx 0.09$), respectively. μ_{ss} is maintained throughout the duration of the test (120 min). Increasing the concentration of ImIL to 5 wt% in PEG further reduces friction marginally, with $\mu_{\max} \approx 0.09$ and $\mu_{ss} \approx 0.083$. The ECR results show that when ImIL is added, the establishment of a stable low friction roughly coincides with the formation of a tribofilm. An ECR of 83% at t = 22 min and 95% at t = 19 min are recorded for 1 wt% and

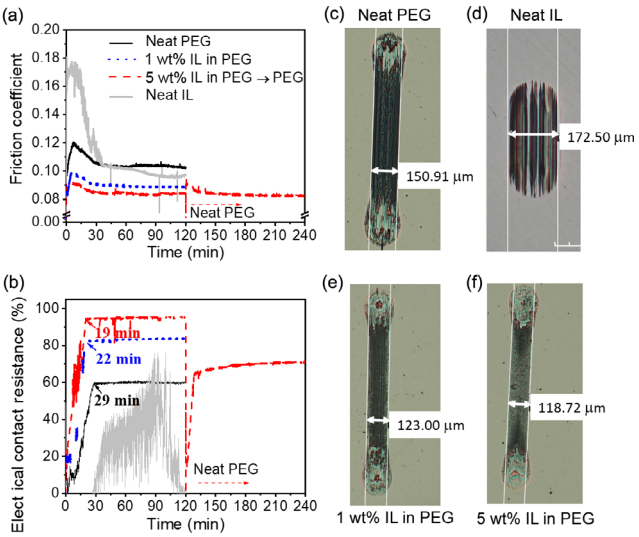

Fig. 3 (a) Friction coefficients, (b) ECR, and (c–f) optical images of wear scars on steel discs formed in PEG with and without IL on steel–steel contacts after rubbing for 120 min. The results of neat IL are included for references.

5 wt% ImIL, respectively. It can be concluded that a higher concentration of ImIL leads to a more effective film in separating the rubbing surfaces formed in a shorter time.

The tribofilm formed in ImIL-containing PEG protects steel rubbing surface from wear, as evident by its narrower and shallower wear scars on rubbed steel discs (Figs. 3(c)–3(f) and Fig. 4). The two ends of the wear track suffer the most wear since the speed at those position is 0. Note that the profiles of wear scars orthogonal to the rubbing direction appear higher than those of the unworn surfaces (Figs. 4(b) vs. 4(c)). This supports the formation of tribofilm. The chemistry of the tribofilm is discussed later.

The integrity of the tribofilm was explored using 5 wt% ImIL-containing PEG. With $\mu_{ss} \approx 0.083$, the test lubricant was exchanged to neat PEG at t = 120 min (Figs. 3(a) and 3(b)). Despite no ImIL in neat PEG, μ_{ss} remains the same for another 120 min. This shows that once the tribofilm is formed, its effectiveness is maintained even after ImIL additives were depleted from the bulk lubricant. This suggests that this tribofilm adheres strongly on the steel surface and maintains its integrity under shear even after ImIL is depleted. It can reduce friction effectively for a prolong period. While μ_{ss} is constant, ECR decreases from above 90% to 68% as ImIL additives are depleted (Fig. 3(b)). This suggests that the tribofilm might have a bilayer structure, with the top layer being removed easily during rubbing and contributes little to reducing friction. The bottom layer of the tribofilm adheres strongly to the rubbing surface and reduces friction.

When neat ImIL is employed as a lubricant, the friction coefficient is very high initially, which falls slowly until reaching a plateau of $\mu_{ss} \approx 0.1$ at $t \approx 38$ min (Fig. 3). At the same time, an ECR value signifies the formation of tribofilm. However, there are considerable fluctuations in the ECR signal, with its maximum reaching around 60%, before dropping to 0% by the end of the test. It results in a very wide scar with deep scratches (Fig. 3(d)). The reason for the poor performance of neat ImIL might be due to the corrosion effect of Cl^- at high concentration [30]. This shows that ImIL works better as an FM additive in

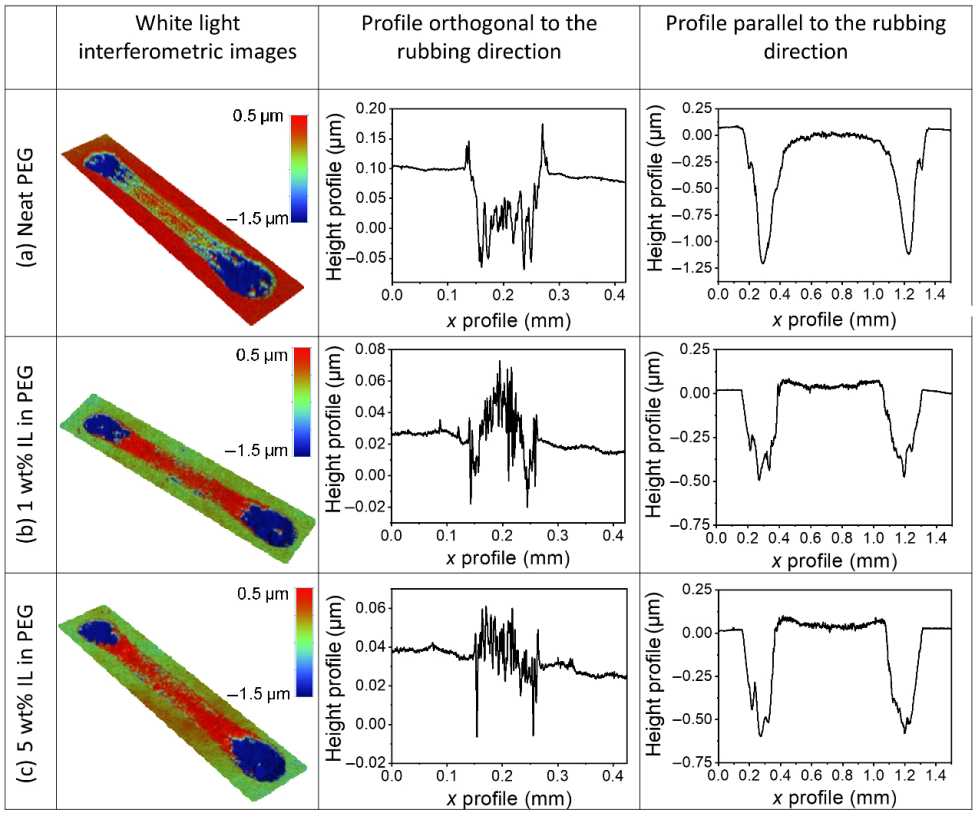

Fig. 4 Profiles of wear scars on steel discs lubricated by (a) neat PEG, (b) 1 wt% ImIL-containing PEG, and (c) 5 wt% ImIL-containing PEG.

PEG than as a neat base fluid. This implies that PEG modifies the interaction between the IL and steel.

5 wt% ImIL in PEG forms a tribofilm readily on DLC, with ECR above 90% almost immediately (Fig. 5(b)). However, this only reduces friction (Fig. 5(a) and Fig. S2(c) in the ESM) and wear on DLC marginally as compared to neat PEG (Figs. 6(a) and 6(b) and Fig. S2(c) in the ESM). This is probably because neat PEG lubricates DLC–DLC contacts well, resulting in low μ_{ss} and little wear in the first place. Interferometric images and profiles of the wear scar, as shown in Fig. S3 in the ESM, do not show an obvious tribofilm, suggesting that the tribofilm may be very thin if it exists.

While ImIL in PEG is effective in lubricating steel–steel contacts, ImIL in 1,4-butanediol does not give a beneficial effect. Adding ImIL into 1,4-butanediol gives a lower initial friction coefficient which increases and eventually results in μ_{ss} higher than that in neat 1,4-butanediol (Fig. 5(c)). The high friction is accompanied by a failure to form a stable tribofilm, as suggested by Fig. 5(d). This results in more severe wear than that observed with neat 1.4-butanediol (Figs. 6(c) and 6(d) and Figs. S3(c) and S3(d) in the ESM). Similar results are also observed with 1,3-propanediol (Figs. S4-1 and S4-2 in the ESM). The results show that ImIL is not an effective FM in diol.

4.2 Surface adsorption of IL

Adsorption of ImIL on Fe_2O_3 and amorphous carbon

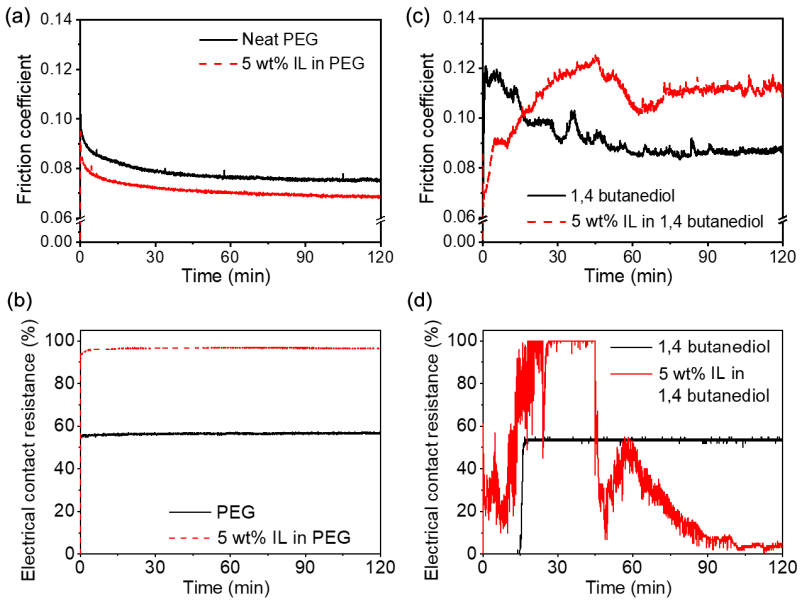

Fig. 5 Friction coefficients and ECR of (a, b) PEG with and without ImIL in DLC–DLC contacts and (c, d) 1,4-butanediol with and without ImIL in steel–steel contacts.

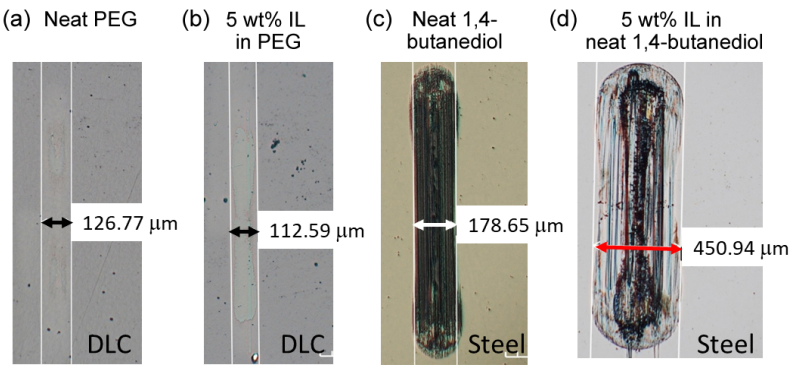

Fig. 6 Optical images showing wear scars formed in (a) neat PEG on a DLC-coated disc, (b) 5 wt% ImIL in PEG on a DLC-coated disc, (c) neat 1,4-butanediol on a steel disc, and (d) 5 wt% ImIL in 1,4-butanediol on a steel disc.

surfaces were examined with QCM-D (Fig. 7). Note that Δf_3 during the flow of ImIL solutions are corrected with liquid loading effect. i.e., the difference in Δf_3 observed during the flow of neat base oils and during the flow of ImIL solutions is due to the adsorption of ImIL.

The introduction of base fluids into the flow cell results in a large Δf_3 (> 2,000 Hz). When the base fluid is replaced with a lubricant containing 5 wt% ImIL, Δf_3 drops slightly further. This is attributed to ImIL adsorption. Similar Δf_3 drop (~40 Hz) due to the introduction of 5 wt% ImIL are observed on Fe_2O_3 (Fig. 7(a)) and carbon surfaces (Fig. 7(b)), indicating similar amount of adsorbed ImIL on these surfaces in PEG. In contrast, a smaller Δf_3 drop of ~20 Hz is detected when 1,4-butanediol is used as the base fluid (Fig. 7(c)). Using the Sauerbrey equation and a molecular weight of 280.5 g/mol, the surface number densities of ImIL on steel in PEG and 1,4-butanediol are 5.06 and 2.53 molecules/nm^2, respectively. Assuming that all the adsorbed ImIL interacts with the surface directly, and that the length of an ImIL molecule is about 1–2 nm, ImIL may have adopted an upright or tilted conformation in PEG on steel surface. This is supported by molecular dynamics simulation which suggests that ImIL absorbs on to a steel surface through the Si–O side of the molecules (Fig. S5 in the ESM).

Why is the amount of adsorbed ImIL on Fe_2O_3 surface lower in 1,4-butanediol than that in PEG? One possibility would be that base fluids compete with ImIL for surface adsorption. Note that 1,4-butanediol and PEG have similar viscosity but different polarity. To investigate this, the adsorption of PEG and 1,4-butanediol in aqueous solutions on Fe_2O_3 surface was examined, as shown in Fig. 8. Numbers in Fig. 8 show the concentrations of base fluids in these aqueous solutions that the sensor was exposed

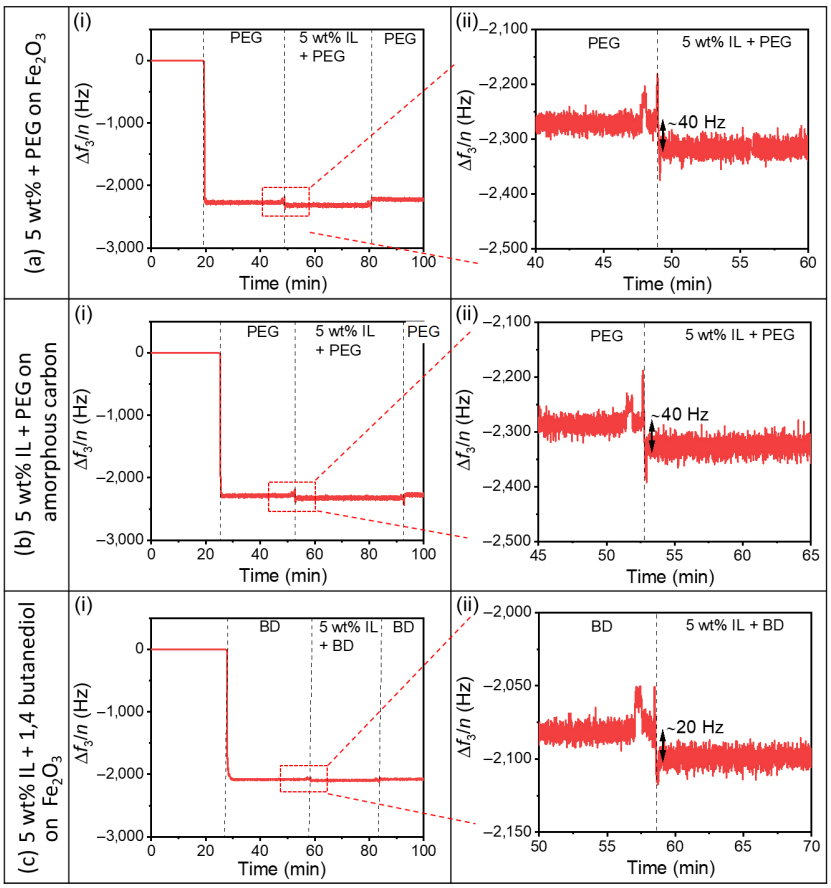

Fig. 7 Introduction of 5 wt% ImIL affects the frequency shift observed in a QCM-D experiment. (i) Δf_3 obtained of the whole flow experiment, (ii) Δf_3 focusing around time ImIL is introduced. Baseline zero is established with IPA. Δf_3 during the flow of ImIL solutions are corrected with liquid loading effect. BD in (c) represents 1,4 butanediol. The fluid that the crystal was exposed to is stated in Fig. 7.

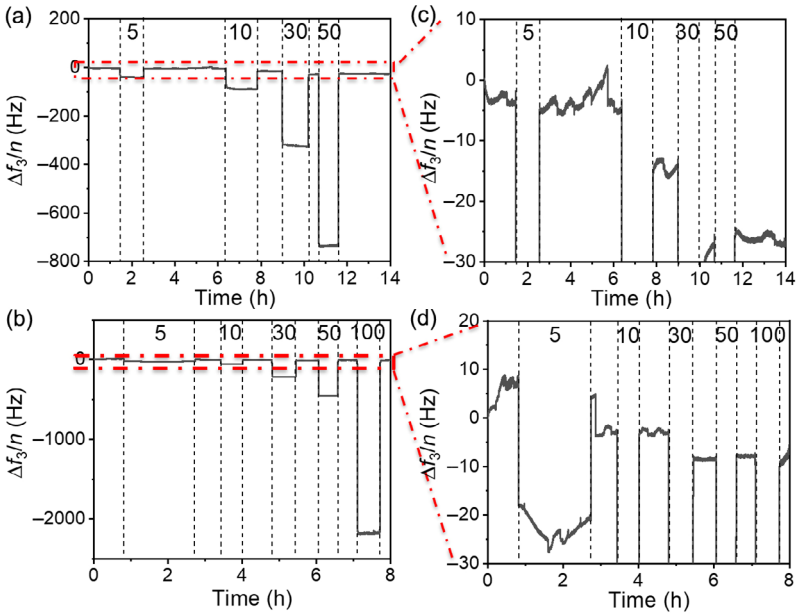

Fig. 8 Δf_3 of a Fe_2O_3-coated sensor due to: (a, c) the flow of aqueous solutions of PEG and (b, d) aqueous solution of 1,4-butanediol. "5", "10", "30", "50", and "100" in Fig. 8 denote the concentrations of a base fluid (in wt%) in water. The baselines were obtained from water. The cell was rinsed with water between the flow of different aqueous solutions. Note that (c, d) are the magnified view of the area highlighted by Rectangles in (a, b).

to at a particular period. The period in between is a rinse step by water whose Δf_3 shows the amount of base fluid molecules remained on the sensor surface during rinsing.

The adsorption of PEG and 1,4-butanediol on a Fe_2O_3 coated sensor results in a maximum Δf_3 shift during water rinsing of ~26 and ~10 Hz, respectively. Using the Sauerbrey equation, this corresponds to an adsorbed mass of 153.4 and 59 ng/cm^2, i.e., a surface number density of 2.31 PEG molecules/nm^2 and 3.91 1,4-butanediol molecules/nm^2, respectively. These results show that 1,4-butanediol adsorbs relatively strongly on Fe_2O_3. As a result, ImIL may not be able to displace the adsorbed 1,4-butanediol effectively, resulting in reduced ImIL adsorption on steel in 1,4-butanediol, as shown in Fig. 7(c). This may explain the poor performance of ImIL in 1,4-butanediol in steel–steel contacts. Together with the friction and wear results in Section 4.1, the combination of base fluids and surfaces that allows a stronger ImIL adsorption gives lower friction and surface wear.

4.3 Chemistry of the IL tribofilms

To examine the chemistry of ImIL tribofilm, Raman spectra of wear tracks were obtained, as shown in Fig. 9. Compared to the spectrum of a clean steel disc before friction test ("A"), the spectrum of the wear track lubricated with neat PEG ("B") displays two distinctive peaks at 663 and 1,327 cm^{-1}, which are assigned to iron nitride/iron oxides and amorphous carbon, respectively [31–35]. Note that the intensity ratio of carbon to iron nitride/iron oxides (I_C/I_{Fe}) was

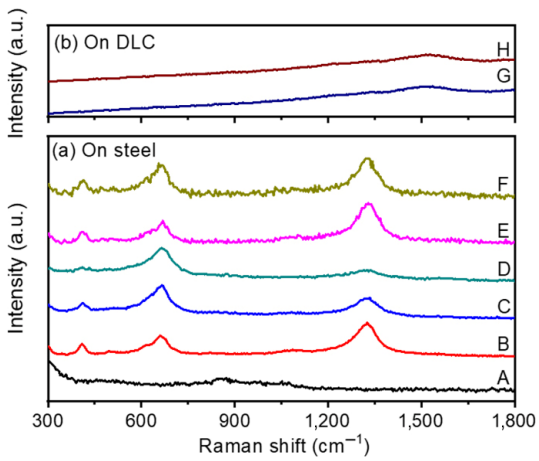

Fig. 9 Raman spectra on steel surfaces: (A) fresh steel surface before friction test and wear track lubricated with (B) PEG, (C) 5 wt% ImIL in PEG, (D) 5 wt% ImIL in PEG followed by neat PEG, (E) 1,4-butanediol, and (F) 5 wt% IL in 1,4-butanediol. (b) Raman spectra on DLC surfaces lubricated with (G) PEG and (H) 5 wt% ImIL in PEG.

greater than 1, indicating that the tribofilm contains a significant amount of carbon. The Raman spectrum obtained on the wear scar formed in 5 wt% ImIL in PEG ("C") also shows these two peaks but its I_C/I_{Fe} is less than 1. This shows that the introduction of ImIL favors (1) the formation of iron nitride or iron oxides or (2) the removal of amorphous carbon. This suggests that an increased iron nitride/iron oxide content or a reduced amorphous carbon content of a tribofilm contributes to an improvement on the tribological performance of a lubricant [36–39].

The Raman spectrum of the wear track exposed to first 5 wt% IL in PEG followed by neat PEG ("D") shows a lower I_C/I_{Fe} than the one using only 5 wt% IL in PEG. Together with the result obtained with ECR shown in Fig. 3(b), this supports that the tribofilm formed in ImIL-containing PEG has a bilayer structure. The top of the tribofilm has more amorphous carbon. This carbon-rich top layer is removed when the tribofilm is rubbed in neat PEG, exposing the bottom layer, which remains intact throughout the rubbing test. It is this bottom layer that gives rise to low friction.

Raman spectra obtained from wear tracks lubricated with 1,4-butanediol with and without 5 wt% ImIL are similar to those lubricated with neat PEG, with I_C/I_{Fe} greater than 1. This indicates that the tribofilms formed by 1,4-butanediol with and without 5 wt% ImIL on steel surfaces, if exist, are carbon rich. One may argue that the use of 5 wt% ImIL in 1,4-butanediol ("F") gives a slightly higher I_C/I_{Fe} than that using neat 1,4-butanediol ("E"). As a carbon-rich film does not seem to offer protection, our result here is consistent with the observations that the use of ImIL in 1,4-butanediol results in worse tribological performance. Raman spectra of DLC wear tracks lubricated with and without ImIL in PEG ("H" and "G" in Fig. 9(b)) are mostly featureless, manifesting that no or limited tribofilm formation. This might be related with the chemical inertness of the carbon [24, 40].

4.4 Chemical analysis of ImIL tribofilms formed in PEG on steel

Since the tribofilm formed on steel by ImIL in PEG offers good tribological performance, its chemistry is further investigated with XPS, FIB-TEM, and AFM.

4.4.1 XPS

XPS spectra obtained from steel wear tracks formed in neat PEG, 5 wt% ImIL in PEG, and ImIL-depleted PEG (rubbed in 5wt% ImIL in PEG for 2 h, followed by neat PEG for another 2 h) are shown in Fig. 10. The C 1s spectra (Fig. 10(a)) exhibit three distinctive peaks at 283.0, 284.8, and 288.4 eV, which are ascribed to Fe–C bond from steel, C–C/C–H bond, and C–O bond, respectively [41, 42]. Note that the spectrum of the wear scar formed in PEG presents the strongest C–O peak, followed by that in 5 wt% ImIL in PEG, and then that in ImIL-depleted PEG. Recall that based on the results from QCM-D (Section 4.2), both PEG and ImIL interact with steel, forming an adsorbed layer. If the Si–O bond in ImIL is hydrolyzed during friction, ImIL may form a chemically-bonded film on surface [43] (Fig. 10(e)). As a result, adsorbed PEG on the surface is replaced, reducing the amount of C–O on the surface. This film is likely to be very thin.

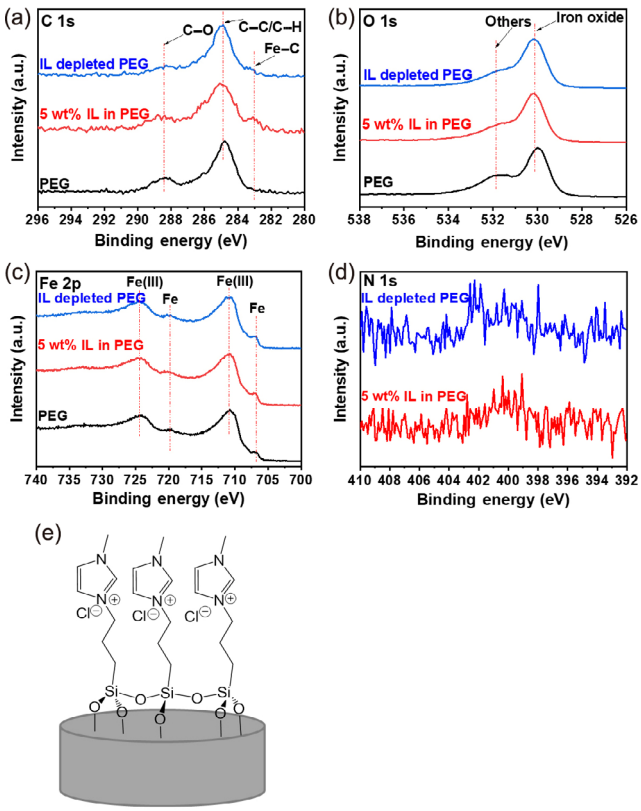

Fig. 10 (a–d) XPS spectra of the wear tracks on steel surface lubricated by PEG, 5 wt% ImIL in PEG, and ImIL-depleted PEG; (e) schematics showing one possible arrangement of ImIL anchored on a steel surface.

The O 1s spectra (Fig. 10(b)) show peaks at 530.1 and 531.9 eV, which are related with iron oxide and other possible components including C–O and C=O [44]. Note that the intensities of the peak at 531.9 eV in the spectra of wear scars formed in 5 wt% ImIL in PEG and ImIL-depleted PEG are lower than that of neat PEG, indicating the removal of C–O and C=O relating compound. This observation is consistent with smaller C–O peaks at 288.4 eV in their C 1s spectra.

In their Fe 2p spectra (Fig. 10(c)), the peaks at 710.9 and 724.5 eV can be assigned to Fe $2p_{3/2}$ and Fe $2p_{1/2}$ in iron nitride/iron oxides, while the peaks at 706.8 and 720.0 eV to Fe $2p_{3/2}$ and Fe $2p_{1/2}$ of Fe [17, 42, 45]. Their N 1s spectra, although weak, show a broad peak around 398–402 eV, which can be contributed to imidazolium ring, nitrogen oxide, and/or Fe(NO_2) compound [37, 45]. Our results suggest that the tribofilm formed in ImIL-containing PEG consists of iron oxide/iron nitride and nitride compound.

The C 1s spectra of wear tracks formed in 1,4-butanediol with and without ImIL show no notable difference in their C–O peaks (Fig. S6(a) in the ESM). This is consistent with the QCM-D results, showing that ImIL only have limited adsorption on steel in 1,4-butandiol. Note that ImIL may react with 1,4-butanediol due to alcoholysis reaction [46, 47]. This may also further reduce the amount of adsorbed ImIL on steel. The resulting tribofilm, if exists, is very thin and offers no protection to steel (Section 4.1).

4.4.2 *FIB-TEM*

The tribofilm on the wear track formed in 5 wt% ImIL in PEG was examined with the FIB-TEM. It was sectioned and observed on the *y*–*z* plane, as shown in Fig. 11(a). A tribofilm is clearly identified (Fig. 11(b)). It has a two-layer structure (Figs. 11(c) and 11(d)), a top amorphous carbon layer and a tribo-boundary film. The EDS-element profiles, scanning from the carbon layer to the underlying steel, show that the tribo-boundary film is about 10–20 nm thick and contains O, Fe, N, and Si (Fig. 11(f)). The existence of N confirms that the tribo-boundary film is IL-related. This also indicates the presence of iron oxide and nitride compound [17, 37] and supports the observations by XPS. These compounds bond strongly to the surface, and can reduce friction and wear effectively [37, 48]. A bilayer tribofilm has been reported in other IL FMs [17], and the thickness of our tribo-boundary film is consistent with the observations from the literature [45]. Note that the materials underneath the tribofilm, which mainly consists of Fe and O, are ordered and aligned to sliding direction (Fig. 11(e)). This may stem from lattice plane rearrangement under shear and may reduce friction [49–51].

4.4.3 *AFM*

The morphology of the tribofilm formed on steel in 5 wt% ImIL in PEG was examined with AFM in contact mode (Fig. 12). The height images (Figs. 12(a)

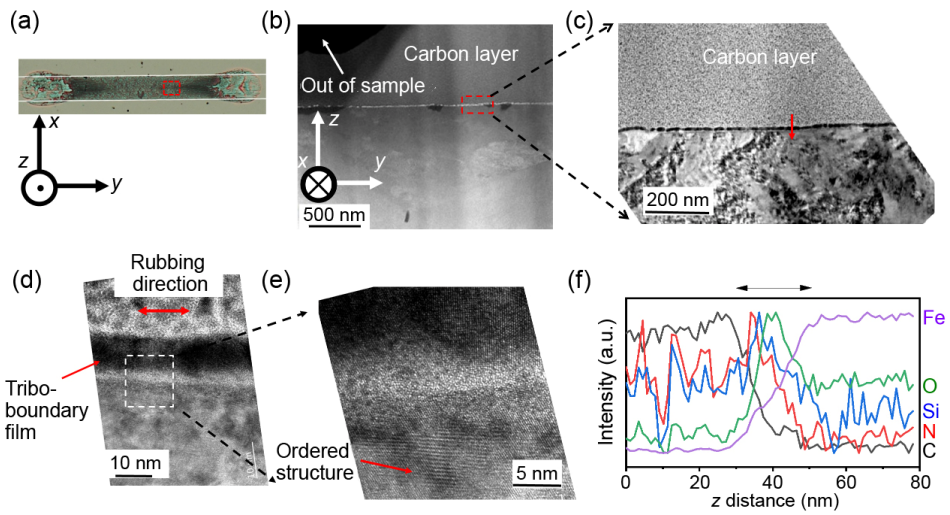

Fig. 11 Results from FIB-TEM of a wear track on steel lubricated by 5 wt% ImIL in PEG: (a) optical micrograph of a wear track on the *x*–*y* plane showing the location where FIB-TEM was performed (rectangle). (b–e) TEM micrographs at various magnifications taken on the *y*–*z* plane and (f) EDS element profiles along the red arrow in (c). The double-arrow line indicates the location of the boundary film.

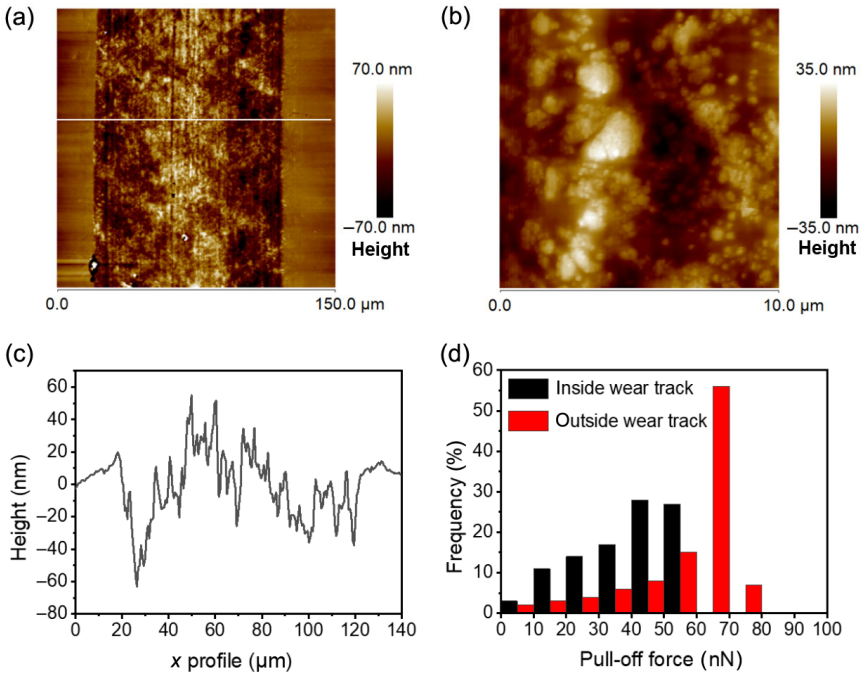

Fig. 12 Height images of the wear track on steel surface lubricated with 5 wt% ImIL in PEG with the scanning sizes of (a) 150 μm and (b) 10 μm. (c) Height profile along the white line in (a). (d) Pull-off forces obtained inside and outside wear track.

and 12(b)) and the cross-section profile (Fig. 12(c)) of the wear track show that the centre of the wear track appears 20–40 nm higher than that of the unrubbed area. This is consistent with the profile obtained using white light interferometer (Fig. 4(c)) and the boundary film thickness obtained in FIB-TEM (Fig. 11(f)). Note that the IL tribofilm consists of irregular islands (Fig. 12(b)), as observed in the previous reports [52, 53].

The adhesion between the AFM tip and the ImIL tribofilm was assessed by measuring the pull-off force necessary to separate the tip from the film after its approach. 100 locations were examined both inside and outside the wear track. The distributions of their pull-off forces are shown in Fig. 12(d). A lower pull-off force is obtained inside the wear track, indicating that a lower adhesion force between the AFM tip and the tribofilm. This supports that the ImIL tribofilm formed on steel in PEG can lead to low friction.

4.5 Proposed IL working mechanism

A summary of the observations is listed in Table 3. The effectiveness of ImIL FM depends on the choice of base fluids and rubbing surfaces. Our results support that ImIL gives an effective and resilient tribofilm on steel in PEG.

The lubricating mechanism of the 5 wt% ImIL in PEG on steel is proposed. Both base fluids (PEG and 1,4-butandiol) can adsorb on the steel surface, as confirmed by the QCM-D results. In PEG, ImIL can adsorb on steel. It is possible that rubbing further promotes its adsorption. Increased surface concentration of ImIL may allow them to form a brush structure [43, 54]. This forms the initial tribo-boundary film which continues to grow until a steady state thickness is reached. Once the tribofilm is formed, it reduces friction effectively even when ImIL is depleted from the lubricant. This tribofilm is tens of nanometer thick. It has an island-like morphology and low adhesion, and hence low friction against rubbing. It is likely that it consists of two layers. The top layer contains more carbon than the bottom layer. It can be removed if ImIL is depleted in the lubricant and contributes little to friction reduction. In contrast, the bottom layer is mainly composed of iron oxide/iron nitride and nitride compound, and adheres strongly on the steel surface to reduce friction effectively.

Note that the adsorbed ImIL film is much thinner than and is of a different chemistry to the tribofilm formed during rubbing. However, the adsorbed film is likely to be important for the subsequent formation of

Table 3 Summary on friction test results and surface analysis on steel surfaces—PEG and 1,4-butanediol with and without IL.

		PEG	5 wt% IL in PEG	IL-depleted PEG	1,4-butanediol	5 wt% IL in 1,4-butanediol
Friction coefficient		0.11	0.083	0.083	0.09	0.11
		ImIL is an effective FM in PEG but not in 1,4-butanediol.				
ECR		60%	95%	68%	50%	0%
		IL-depleted PEG exhibits a stable higher ECR than neat PEG, but lower than IL-containing PEG, indicating a bilayer structure of tribofilm. Adding ImIL in 1,4-butanediol cannot contribute to tribofilm formation.				
Wear track width (μm)		150.91	123.00	118.72	178.65	450.94
		ImIL forms rough film (tens of nanometer thick) and offers some wear protection in PEG. ImIL in 1,4-butanediol offers no wear protection.				
QCM (surface number density, nm^2)	ImIL in base fluids: based on Δf during adsorption	—	5.06	—	—	2.53
		ImIL has a stronger affinity to steel in PEG than in butanediol. Adsorbed ImIL are removed during rinsing.				
	Base fluids: based on Δf during rinsing in water	2.31	—	—	3.94	—
		Both base fluids adsorb on steel, with 1,4-butanediol having a stronger affinity.				
Raman I_C/I_{Fe}		> 1	< 1	<< 1	> 1	> 1
		Tribofilm by ImIL in PEG consists of two layers. The top layer is carbon rich and is easily to be removed, while the bottom is iron oxide or iron nitride rich. Tribofilm by ImIL in 1,4 butanol, if exists, is carbon rich.				
XPS		High C–O	Low C–O and weak N signal	Very low C–O	High C–O	High C–O
		ImIL replaces the adsorbed PEG on steel under rubbing. The bottom layer may have more ImIL than the top layer. No change in the interaction between 1,4-butanediol and steel with the addition of ImIL.				
FIB-TEM		—	Tribofilm with bilayer structure observed	—	—	—
		The top of the film is carbon rich, while the bottom is iron oxide/iron nitride rich.				
AFM		—	Islands with low adhesion force	—	—	—
		Island-like tribofilm (tens of nm thick) is observed and possesses low adhesion, suggesting that it has low friction.				

the tribofilm. This is supported by the results obtained with ImIL in 1,4-butanediol, where low ImIL adsorption on steel links to poor wear performance.

5 Conclusions

An imidazolium ionic liquid (ImIL) was synthesized and employed as a friction modifier (FM). The compatibility of this FM with different base fluids (PEG and 1,4-butanediol) on different surfaces (steel and DLC) was investigated. ImIL is an effective FM in PEG for a steel–steel contact but offers little benefit in a DLC–DLC contact. The effectiveness of ImIL in PEG on steel surface can be attributed to the tribofilm that forms during rubbing. The tribofilm has a two-layer structure. The top layer can be easily removed during the rubbing, while the bottom layer, which is composed of iron oxide/iron nitride and nitride compound, adheres strongly on the steel rubbing surfaces.

DLC surface is hard and can be lubricated by neat PEG well. It is also chemically inert, so ImIL cannot adsorb and form a tribofilm. ImIL in 1,4-butanediol performs poorly in steel–steel contacts. QCM results

suggest that in this case, ImIL does not have strong affinity to steel. This may stem from its inability to displace 1,4-butanediol adsorbed on steel. ImIL and 1,4-butanediol may also interact in the bulk solution.

While it is intuitive that the interaction between the surface and the additive is crucial to the performance of a surface-active additive such as ImIL FM, the study shows that the role of base fluid cannot be overlooked. Base oil can alter the performance of additive by (1) competitive adsorption or (2) interacting with the additive in the solution. Both factors must be considered, on top of the compatibility between the surface and the additive, to ensure an appropriate selection of lubricant.

Acknowledgements

Wei SONG is supported by China Scholarship Council. The authors would like to thank Dr. Gwilherm KERHERVE of the Advanced Photoelectron Spectroscopy Laboratory, Imperial College London, for his help with XPS. The authors would also like to acknowledge the support from Imperial College Research Computing Service (https://doi.org/10.14469/hpc/2232).

Declaration of competing interest

The authors have no competing interests to declare that are relevant to the content of this article.

Electronic Supplementary Mayerial Supplementary material is available in the online version of this article at https://doi.org/10.1007/s40544-022-0614-9.

References

[1] Bronshteyn L A, Kreiner J H. Energy efficiency of industrial oils. *Tribol Trans* **42**(4): 771–776 (1999)

[2] Hsu S M, Zhang J, Yin Z F. The nature and origin of tribochemistry. *Tribol Lett* **13**(2): 131–139 (2002)

[3] Boyde S. Green lubricants. Environmental benefits and impacts of lubrication. *Green Chem* **4**(4): 293–307 (2002)

[4] Spikes H. Friction modifier additives. *Tribol Lett* **60**: 5 (2015)

[5] Zhang J, Meng Y G. Boundary lubrication by adsorption film. *Friction* **3**(2): 115–147 (2015)

[6] Mordukhovich G, Qu J, Howe J Y, Bair S, Yu B, Luo H M, Smolenski D J, Blau P J, Bunting B G, Dai S. A low-viscosity ionic liquid demonstrating superior lubricating performance from mixed to boundary lubrication. *Wear* **301**(1–2): 740–746 (2013)

[7] Desanker M, He X L, Lu J, Liu P Z, Pickens D B, Delferro M, Marks T J, Chung Y W, Wang Q J. Alkyl-cyclens as effective sulfur- and phosphorus-free friction modifiers for boundary lubrication. *ACS Appl Mater Interfaces* **9**(10): 9118–9125 (2017)

[8] Bassanetti I, Twist C P, Kim M G, Seyam A M, Bazzi H S, Wang Q J, Chung Y W, Marchió L, Delferro M, Marks T J. Synthesis and characterization of silver(I) pyrazolylmethylpyridine complexes and their implementation as metallic silver thin film precursors. *Inorg Chem* **53**(9): 4629–4638 (2014)

[9] Li K, Amann T, List M, Walter M, Moseler M, Kailer A, Rühe J. Ultralow friction of steel surfaces using a 1,3-diketone lubricant in the thin film lubrication regime. *Langmuir* **31**(40): 11033–11039 (2015)

[10] Zhou Y, Qu J. Ionic liquids as lubricant additives: A review. *ACS Appl Mater Interfaces* **9**(4): 3209–3222 (2017)

[11] Zhou F, Liang Y M, Liu W M. Ionic liquid lubricants: Designed chemistry for engineering applications. *Chem Soc Rev* **38**(9): 2590–2599.

[12] Qu J, Luo H M, Chi M F, Ma C, Blau P J, Dai S, Viola M B. Comparison of an oil-miscible ionic liquid and ZDDP as a lubricant anti-wear additive. *Tribol Int* **71**: 88–97 (2014)

[13] Zhou Y, Weber J, Viola M B, Qu J. Is more always better? Tribofilm evolution and tribological behavior impacted by the concentration of ZDDP, ionic liquid, and ZDDP-ionic liquid combination. *Wear* **432–433**: 202951 (2019)

[14] Yu Q L, Zhang C Y, Dong R, Shi Y J, Wang Y R, Bai Y Y, Zhang J Y, Cai M R, Zhou F, Liu W M. Physicochemical and tribological properties of gemini-type halogen-free dicationic ionic liquids. *Friction* **9**(2): 344–355 (2021)

[15] Qu M H, Yang Z Q, Zhang C Y, Yu Q L, Cai M R, Zhou F. Significantly enhancing lubricity and anti-wear performances of glycerol lubricant with urea-functionalized imidazolium-organophosphate ionic liquid as additive. *Tribol Int* **153**: 106602 (2021)

[16] Cai M R, Yu Q L, Liu W M, Zhou F. Ionic liquid lubricants: When chemistry meets tribology. *Chem Soc Rev* **49**(21): 7753–7818 (2020)

[17] Li W M, Kumara C, Luo H M, Meyer H M III, He X, Ngo D, Kim S H, Qu J. Ultralow boundary lubrication friction by three-way synergistic interactions among ionic liquid, friction modifier, and dispersant. *ACS Appl Mater Interfaces* **12**(14): 17077–17090 (2020)

[18] Li W M, Kumara C, Meyer H M III, Luo H M, Qu J. Compatibility between various ionic liquids and an organic friction modifier as lubricant additives. *Langmuir* **34**(36): 10711–10720 (2018)

[19] Guegan J, Southby M, Spikes H. Friction modifier additives, synergies and antagonisms. *Tribol Lett* **67**(3): 83 (2019)

[20] Ngo D, He X, Luo H M, Qu J, Kim S H. Competitive adsorption of ionic liquids versus friction modifier and anti-wear additive at solid/lubricant interface—Speciation with vibrational dum frequency generation spectroscopy. *Lubricants* **8**(11): 98 (2020)

[21] Neville A, Morina A, Haque T, Voong M. Compatibility between tribological surfaces and lubricant additives—How friction and wear reduction can be controlled by surface/lube synergies. *Tribol Int* **40**(10–12): 1680–1695 (2007)

[22] Hanna F F, Gestblom B, Soliman A. Dielectric relaxation study of alcohol/diol(s) mixtures. *J Mol Liq* **95**(1): 27–40 (2002)

[23] Fujimori Y, Kaden W E, Brown M A, Cuenya B R, Sterrer M, Freund H J. Hydrogen evolution from metal–surface hydroxyl interaction. *J Phys Chem C* **118**(31): 17717–17723 (2014)

[24] Grill A. Review of the tribology of diamond-like carbon. *Wear* **168**(1–2): 143–153 (1993)

[25] Dou Q Y, Liu L Y, Yang B J, Lang J W, Yan X B. Silica-grafted ionic liquids for revealing the respective charging behaviors of cations and anions in supercapacitors. *Nat Commun* **8**: 2188 (2017)

[26] Viesca J L, Battez A H, González R, Reddyhoff T, Pérez A T, Spikes H A. Assessing boundary film formation of lubricant additivised with 1-hexyl-3-methylimidazolium tetrafluoroborate using ECR as qualitative indicator. *Wear* **269**(1–2): 112–117 (2010)

[27] Hamrock B J, Dowson D. Isothermal elastohydrodynamic lubrication of point contacts: Part III—Fully flooded results. *J Lubr Technol* **99**(2): 264–275 (1977)

[28] Tavakkoli M, Panuganti S R, Vargas F M, Taghikhani V, Pishvaie M R, Chapman W G. Asphaltene deposition in different depositing environments: Part 1. Model oil. *Energy Fuels* **28**(3): 1617–1628 (2014)

[29] Campen S, Smith B, Wong J. Deposition of asphaltene from destabilized dispersions in heptane–toluene. *Energy Fuels* **32**(9): 9159–9171 (2018)

[30] Quraishi M A, Nayak D K, Kumar R, Kumar V. Corrosion of reinforced steel in concrete and its control: An overview. *J Steel Struct Constr* **3**(1): 1000124. (2017)

[31] Wu H X, Khan A M, Johnson B, Sasikumar K, Chung Y W, Wang Q J. Formation and nature of carbon-containing tribofilms. *ACS Appl Mater Interfaces* **11**(17): 16139–16146 (2019)

[32] De Faria D L A, Venâncio Silva S, de Oliveira M T. Raman microspectroscopy of some iron oxides and oxyhydroxides. *J Raman Spectrosc* **28**(11): 873–878 (1997)

[33] Hanesch M. Raman spectroscopy of iron oxides and (oxy)hydroxides at low laser power and possible applications in environmental magnetic studies. *Geophys J Int* **177**(3): 941–948 (2009)

[34] Berman D, Erdemir A, Sumant A V. Reduced wear and friction enabled by graphene layers on sliding steel surfaces in dry nitrogen. *Carbon* **59**: 167–175 (2013)

[35] Berman D, Erdemir A, Sumant A V. Few layer graphene to reduce wear and friction on sliding steel surfaces. *Carbon* **54**: 454–459 (2013)

[36] Totolin V, Göcerler H, Rodríguez Ripoll M, Jech M. The role of ferric oxide nanoparticles in improving lubricity and tribo-electrochemical performance during chemical–mechanical polishing. *Tribol Lett* **65**(1): 20 (2017)

[37] Han Y Y, Qiao D, Guo Y X, Feng D P, Shi L. Influence of competitive adsorption on lubricating property of phosphonate ionic liquid additives in PEG. *Tribol Lett* **64**(2): 22 (2016)

[38] Iida S, Hidaka Y. Influence of the iron oxide layer on lubricating properties in seamless pipe hot rolling. *Tetsu-to-Hagane* **94**(7): 244–250 (2008)

[39] Hu Z S, Dong J X, Chen G X. Study on antiwear and reducing friction additive of nanometer ferric oxide. *Tribol Int* **31**(7): 355–360 (1998)

[40] Fiaschi G, Rota A, Ballestrazzi A, Marchetto D, Vezzalini E, Valeri S. A chemical, mechanical, and tribological analysis of DLC coatings deposited by magnetron sputtering. *Lubricants* **7**(4): 38 (2019)

[41] Ge X Y, Li J J, Zhang C H, Liu Y H, Luo J B. Superlubricity and antiwear properties of *in situ*-formed ionic liquids at ceramic interfaces induced by tribochemical reactions. *ACS Appl Mater Interfaces* **11**(6): 6568–6574 (2019)

[42] Xu Y F, Peng Y B, Dearn K D, Zheng X J, Yao L L, Hu X G. Synergistic lubricating behaviors of graphene and MoS_2 dispersed in esterified bio-oil for steel/steel contact. *Wear* **342–343**: 297–309 (2015)

[43] Wu B N, Breen J P, Xing X Y, Fayer M D. Controlling the dynamics of ionic liquid thin films via multilayer surface functionalization. *J Am Chem Soc* **142**(20): 9482–9492 (2020)

[44] Zhou Y, Dyck J, Graham T W, Luo H M, Leonard D N, Qu J. Ionic liquids composed of phosphonium cations and organophosphate, carboxylate, and sulfonate anions as lubricant antiwear additives. *Langmuir* **30**(44): 13301–13311 (2014)

[45] Dong R, Yu Q L, Bai Y Y, Wu Y, Ma Z F, Zhang J Y, Zhang C Y, Yu B, Zhou F, Liu W M, et al. Towards superior lubricity and anticorrosion performances of proton-type ionic liquids additives for water-based lubricating fluids. *Chem Eng J* **383**: 123201 (2020)

[46] Lukevics E, Dzintara M. The alcoholysis of hydrosilanes. *J Organomet Chem* **295**(3): 265–315 (1985)

[47] Oostendorp D J, Bertrand G L, Stoffer J O. Kinetics and mechanism of the hydrolysis and alcoholysis of alkoxysilanes. *J Adhesion Sci Technol* **6**(1): 171–191 (1992)

[48] Khan T, Koide S, Tamura Y, Yamamoto H, Morina A, Neville A. Effects of using alternative extreme pressure (EP) and anti-wear (AW) additives with oxy-nitrided samples. *Tribol Lett* **66**(1): 43 (2018)

[49] Zhao J, Mao J Y, Li Y R, He Y Y, Luo J B. Friction-induced nano-structural evolution of graphene as a lubrication additive. *Appl Surf Sci* **434**: 21–27 (2018)

[50] Taylor G I. The mechanism of plastic deformation of crystals. Part I.—Theoretical. *Proc Roy Soc A Mat Phys Eng Sci* **145**(855): 362–387 (1934)

[51] Anderson J S, Tilley R J D. Crystallographic shear in oxygen-deficient rutile: An electron microscope study. *J Solid State Chem* **2**(3): 472–482 (1970)

[52] Zhang J, Spikes H. On the mechanism of ZDDP antiwear film formation. *Tribol Lett* **63**(2): 24 (2016)

[53] Gosvami N N, Bares J A, Mangolini F, Konicek A R, Yablon D G, Carpick R W. Mechanisms of antiwear tribofilm growth revealed *in situ* by single-asperity sliding contacts. *Science* **348**(6230): 102–106 (2015)

[54] Guo Y X, Zhang L G, Zhang G, Wang D A, Wang T M, Wang Q H. High lubricity and electrical responsiveness of solvent-free ionic SiO_2 nanofluids. *J Mater Chem A* **6**(6): 2817–2827 (2018)

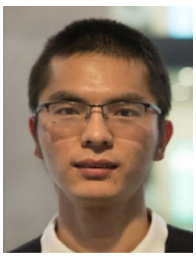

Wei SONG. He received his Ph.D. degree in chemistry in 2021 from Sun Yat-sen University, China. He was a visiting Ph.D. student in Tribology Group in Imperial College London, UK, from November 2019 to October 2021. He recently joined the State Key Laboratory of Tribology in Tsinghua University, China, as a postdoctor. His research interest includes friction modifier (FM) under boundary lubrication.

Jie ZHANG. He received his M.S. degree in tribology and surface engineering from China University of Geosciences (Beijing), China, in 2007. He subsequently joined the Tribology Group in Imperial College London, UK, as a Ph.D. student and completed in 2011. Since 2013, he started to work in the same group as a research associate on different projects. His main research areas cover boundary lubrication, wear, lubricant additives, elasto-hydrodynamic (EHD) lubrication, micro-electro-mechanical system (MEMS), zinc dialkyldithiophosphate (ZDDP), mechanochemistry, and atmospheric tribology.

Sophie CAMPEN. She received her M.S. degree in chemistry and her Ph.D. degree in mechanical engineering from Imperial College London, UK, in 2007 and 2012, respectively. Her current position is the research associate at the University of Cambridge, UK. Her research areas include boundary lubrication, mechanochemistry, and surface adsorption.

Jincan YAN. He received his bachelor degree in chemistry and master's degree in organic chemistry from Huaibei Normal University, China, in 2002 and 2008, respectively, and Ph.D. degree in mechanical engineering from Twente University, the Netherlands, and Ph.D. degree in chemical engineering from Shanghai JiaoTong University, China, in 2014. He is now an associate professor in Shanghai Institute of Technology, China. His research interests include lubricant additives, lubricating oil and grease, cutting fluid, and surface engineering.

Hongbing JI. He received his bachelor degree and Ph.D. degree in chemical engineering from South China University of Technology, China, in 1992 and 1997, respectively. His current position is a professor in Sun Yat-sen University, China. His research areas cover biomimetic catalysis, heterogeneous catalysis, homogeneous catalysis, and lubricant additives.

Janet S. S. WONG. She received her Ph.D. degree from University of Illinois at Urbana-Champaign, USA, in 2008. She is now a senior lecturer in the Tribology Group, Mechanical Engineering Department, Imperial College London, UK. Her research interest covers phenomena at solid–liquid interface, lubricant rheology, additive technology, mechanochemistry, and *in-situ* experimentation development.